The 2017 World Congress on
Advances in Structural Engineering and Mechanics (ASEM17)
28 August - 1 September, 2017, Ilsan(Seoul), Korea

Simulation and analytical of R.C bevel beam with FRP composite in boundary condition method

Tian Zi Eng[1)] and *Peiwei Gao[2)]

Department of Civil Engineering, College of Aerospace Engineering, Nanjing University of Aeronautics and Astronautics, 29 Yudao Street, Nanjing 210016 P.R.China
[1)] *alexia.eng@outlook.com*

ABSTRACT

The 45° bevel edge beam with composite material of rebar and glass-fiber reinforcement polymer (GFRP) is present to discover the discrepancy with perpendicular edge beam through experiment, formula calculation and simulation to find out the performance in flexural strength, stress tensor and failed mode status on the specific composite beam. The modeling of COMSOL Multiphysics by utilization in boundary element method (BEM) is express to evidence the functionality of the bevel edge beam compare with the perpendicular edge beam with the additional GFRP composite material to enhance the utilization of the beam after load application for renovated use. The simulation and analytical result of bevel edge beam shows advantage in flexural strength after receiving the load in soffit compare with the perpendicular edge beam while the comparison of the both experiment and simulation result shows resemblance ≈ 1. Hence, the modeling simulation in COMSOL Multiphysics is competent to simulation the multi-layer composite beam in a short term with enormous quantity while the result shows approaching with the actual experiment status.

1. INTRODUCTION

Bevel edge beam is rarely in used compare with the perpendicular edge beam in building construction while it was normally applying on the link bridge structural. (Axiang Zhu 2017) was indicated the functionality of GFRP retrofitting in 45° bevel edge R.C beam. While, the functionality of glass fiber reinforcement polymers (GFRP) for R.C beam is significantly to precede the serviceability, flexural strength and fatigue life in structural maintenance and renovated. (ACI 440.2R-08 2008),(Hind M. Kh. And etc.) were indicate the FRP bonded system for externally strengthening concrete structural and material maintenance in renovated beam application. (Hany Jawaheri Zadeh and ect. 2013), (Liang Jiongfeng and etc. 2016) was mention about the sequence of

[1)] PhD.
[2)] Professor

material predicted in rebar yielding and FRP rupture modes for the renovated R.C beam in formulation to obtain the accuracy rupture modes in several condition.

Whereas, the formulation for the composite beam is bustling to calculated as manually since the component of each beam is variable. Hence, (Anand Ganganagoudar and etc. 2016), (Zhang Dongliang and etc. 2016) were study the finite element method (FEM) with ABAQUS modeling and indicated the constitutive relationship of concrete, steel and FRP in numerical dispersion error significantly affects the accuracy of numerical results for wave propagation in the vicinity of crack tips. Although the F.E.M simulation was superior and popularization in structural modeling while the limitation in formula compute is an obstacle for research development. (COMSOL Multiphysics 2016) the COMSOL simulation tool is able to simulated with the creation formula especially a new ideal of composite structure. Hence, the modeling simulation of the GFRP composite beam in bevel edge is present to comprehend its performance as well as accuracy verification between the experiment and simulation model.

2. NARRITIVE IN GFRP COMPOSITE BEAM

2.1 Material properties

2-group specimen as 45° bevel edge beam and perpendicular edge beam with 6-beam specimen respectively is show in Fig.1. The rebar for all the specimen in A'_s position is HRB335 as 2B10 while the rebar in the A_s position for L-1-1 to L-1-3 and N-1-1 to N-1-3 is 2B12. The rebar in A_s position for L-2-1 to L-2-3 and N-2-1 to N-2-3 is 2B14. The space gap a and a'_s from the boundary beam to steel rebar is 20mm, the yield strength of rebar is 477.5MPa, the ultimate strength is 621.1MPa and the elastic modulus is 1.96 × 105MPa. GFRP is an elementary fiber glass with 22GPa elastic modulus and 540 MPa tensile Strength with 0.2mm thickness and density 2.5g/cm^3. The ultimate strength of cement concrete is in grade C50 with 34.5GPa elastic modulus and 23.1MPa uniaxial compressive strength with density 2300 kg/m^3.

Specimen L-1-1, L-2-1 and N-1-1, N-2-1 is the control beam for calibration whereas L-1-2, L-2-2 and N-1-2, N-2-2 is the renovated R.C beam without GFRP reinforcement while L-1-3, L-2-3 and N-1-3, N-2-3 is the renovated R.C beam with GFRP reinforcement. The force bearing is set-up as three point symmetric concentrated force as show in Fig.1. The beam failed due to flexural intermedia deboding from the midspan with propagated towards the ends of the beam edge. The control beam (L-1-1, L-2-1 and N-1-1, N-2-1) with the renovated R.C beam without GFRP (L-1-2, L-2-2 and N-1-2, N-2-2) is failed in a typical flexural concrete crushing after yielding of the main tensile steel. While, the renovated R.C beam with GFRP reinforcement L-1-3, L-2-3 and N-1-3, N-2-3 were failed after the GFRP rupture as indicated in (Axiang Zhu 2017) experiment.

Fig. 1 shown the beam parameter with dimensional term for cross-section beam in force equilibrium status. Where, A_s and A'_s is the area of tension and compressive

steel reinforcement (mm^2), A_f is the GFRP external reinforcement area (mm^2). c is the estimated distance of neutral axis (mm). ε_c is the stain level in the concrete, ε_f is the strain level in the FRP reinforcement, ε_{bi} is the strain level in the concrete substrate at the time of the FRP installation. f'_c is the compressive strength of concrete, E_c is the concrete elasticity modulus (MPa), $f_{s,s}$ is the stress level for steel reinforcement (MPa), $f_{f,s}$ is the stress level in the FRP (MPa).

(a) Longitude elevation of bevel beam and perpendicular beam

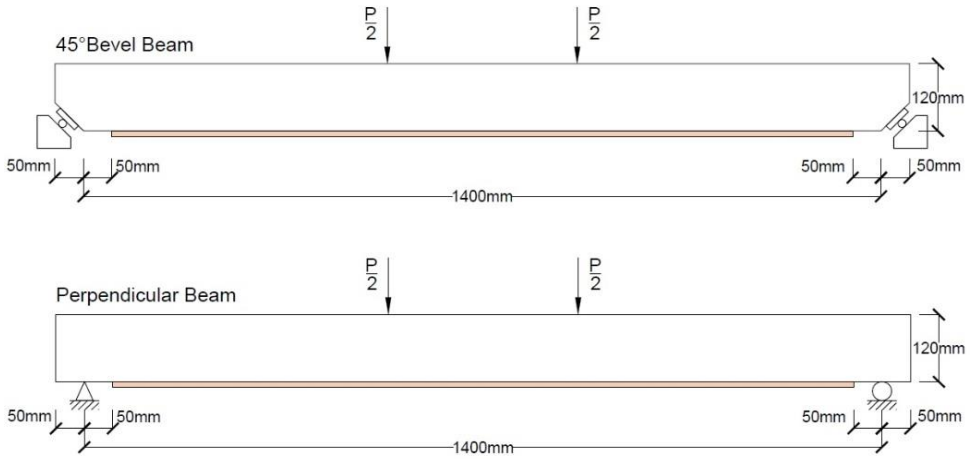

(b) FRP reinforcement beam in compatibility and equilibrium condition

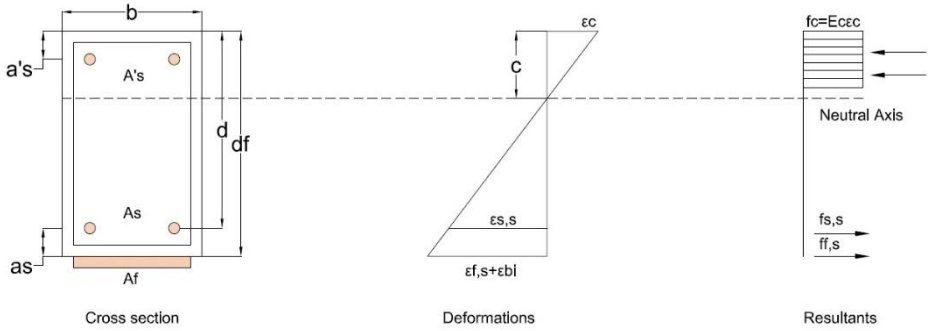

Fig. 1 The equilibrium condition of FRP reinforcement beam

2.2 Experimental result

The specimens result represents by (Axiang Zhu 2017) in 45° bevel edge beam is express as control beam, renovated beam and GFRP reinforcement renovated beam. The failed modes for beam L-1-1 is 50.5kN with 12.52kN·m flexural strength, the beam after renovated L-1-2 is 51kN with 12.75kN·m, the beam after renovated with GFRP composite L-1-3 is rupture in 53kN with 13.25kN·m flexural strength. The control beam for 14mm rebar L-2-1 is 52.5kN with 13.13kN·m, the beam after renovated with 14mm rebar L-2-2 is failed in 54kN with 13.50kN·m and the beam after renovated with GFRP composite and 14mm rebar L-2-3 is failed in 59kN with 14.75kN·m flexural strength.

2.3 Numerical computation procedure

The equilibrium neutral axis is a variable number which be able to adjusted and apply to the Eq.(1) after the supplement of GFRP:

$$c = \frac{A_s f_s - A'_s f'_s + A_f f_{fe}}{\alpha_1 \beta_1 f'_c b} \quad (1)$$

The internal moment M_n is obtain by taking the moments of internal forces about the extreme is indicate from ACI guideline as show in Eq.(2).

$$\phi M_n = \phi \left[A_s f_s \left(d - \frac{\beta_1 c}{2} \right) + \Psi_f A_f f_{fe} \left(d_f - \frac{\beta_1 c}{2} \right) \right] \quad (2)$$

Whereas, the Eq.(2) has limitation to compute for double row rebar in A'_s, f'_s and a'_s. The additional condition according to double row rebar as show in Eqs.(3)-(5):

$$M_n = \phi \left[A_s f_s \left(d - \frac{\beta_1 c_i}{2} \right) + A'_s f'_s a'_s + \Psi_f A_f f_{fe} \left(d_f - \frac{\beta_1 c_i}{2} \right) \right] \quad (3)$$

Since

$A_s \neq A'_s$, Therefore, $f_s \neq f'_s$ (4)

Where

$$f'_s = E_s \varepsilon_s \leq f'_y \qquad \text{Thus,} \qquad f'_y = \frac{\alpha_1 f'_c b c_i}{A'_s} \quad (5)$$

The strength-reduction factor of GFRP in one side wrapping can express as Eq.(6):

$$\Psi_f = \frac{(0.85 \varepsilon_c d_f / c_i) - (\varepsilon_c + \varepsilon_{bi})}{\varepsilon_{fu}} \quad (6)$$

A strength reduction factor ϕ as Eq.(7):

$$\emptyset = \begin{cases} 0.90 \; for \; \varepsilon_t \geq 0.005 \\ 0.65 + \frac{0.25(\varepsilon_t - \varepsilon_{sy})}{0.005 - \varepsilon_{sy}} for \; \varepsilon_{sy} < \varepsilon_t < 0.005 \\ 0.65 \; for \; \varepsilon_t \leq \varepsilon_{sy} \end{cases} \quad (7)$$

The compression of double row rebar and FRP is required for determining in deflection experienced by the beam under flexural loading. Whereas, the intention of stirrups between the rebar is able to ignore since it is not significant in load bearing as indicated in (ACI 440R-08 2008).

3. MODEL SIMULATION

3.1 Load distribution

Composite of 45° Bevel Edge Beam	Composite of Perpendicular Edge Beam
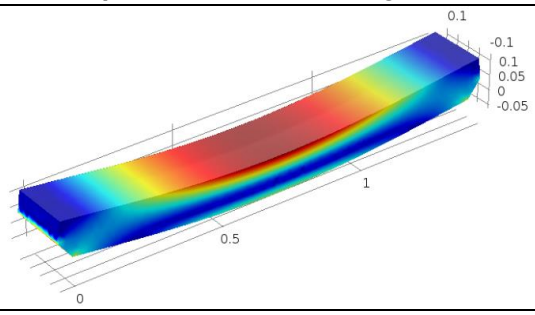	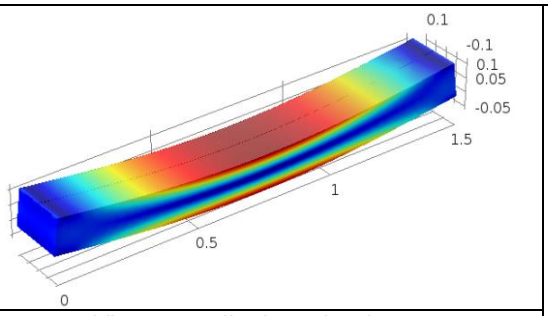
(a) Bevel beam	(d) Perpendicular edge beam
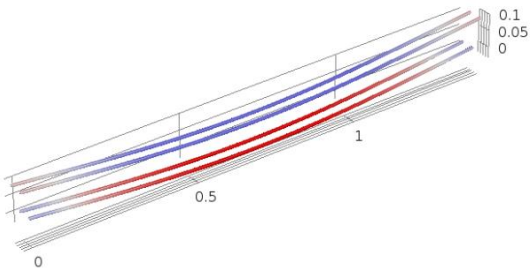	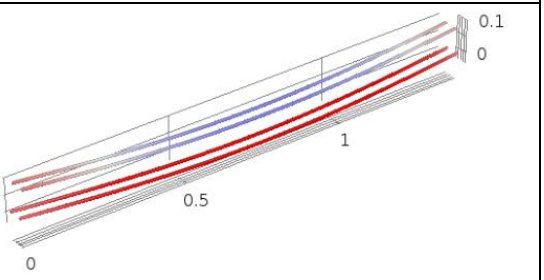
(b) Rebar	(e) Rebar
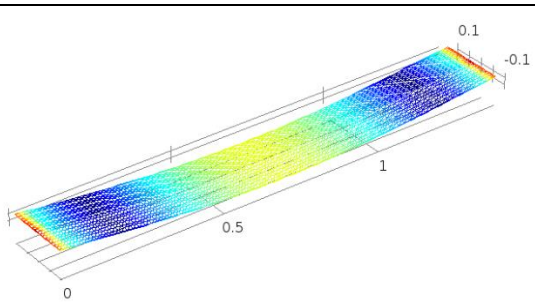	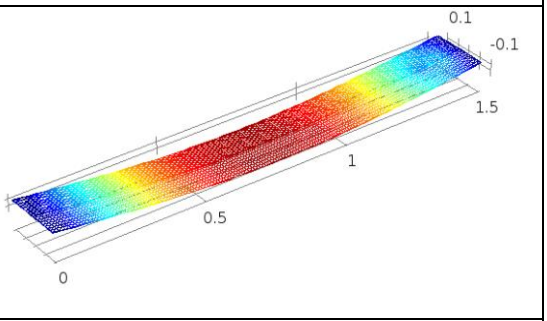
(c) GFRP	(f) GFRP

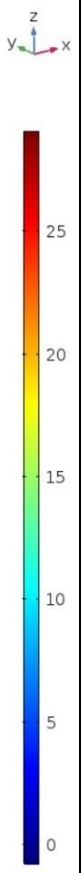

Fig.2 Stress tensor of bevel edge beam and perpendicular edge beam

Fig.2 show the loading stress performance in 45°bevel edge beam L-1-3 and perpendicular edge beam N-1-3. Fig.2(a) show the ultimate force bearing in compressive stress A'_s of the beam and 45° inclination force bearing in both of the beam side while the stress distribution in GFRP for 45°bevel edge beam in the soffit is still able for load bearing as show in Fig.2(c). Whereas, Fig.2(b) show that the yielding forces of the rebar for the compressive stress A'_s and tensile stress in the soffit A_s is in the ultimate mode distributed from the center to the side. The stress distribution for the perpendicular beam is show saturation in load bearing. Where, Fig.2(d) show the ultimate force bearing in the upper part and soffit of the beam after receiving the force bearing. However, the status of the yielding forces of the rebar for compressive stress A'_s is still able in force carried whereas the tensile stress in the soffit for the rebar A_s is in a saturation mode while the GFRP is getting to rupture.

3.2 Stress tensor

Table 1 Stress tensor of 45° bevel beam with GFRP composite

Beam code	Description	Rupture load (kN)	Axial stress (MPa)	M_u(kN)
L-1-1	A_s: 12mm rebar Status: Control-R.C. beam	50.50	Beam: 15.505 Rebar: 101.260 FRP: -	11.20
L-1-2	A_s: 12mm rebar Status: Renovated R.C. beam	51.00	Beam: 15.692 Rebar: 101.340 FRP: -	11.21
L-1-3	A_s: 12mm rebar Status: Renovated R.C. beam with FRP composite	53.00	Beam: 15.671 Rebar: 101.230 FRP: 15.093	12.57
L-2-1	A_s: 14mm rebar Status: Control-R.C. beam	52.50	Beam: 15.743 Rebar: 101.280 FRP: -	14.98
L-2-2	A_s: 14mm rebar Status: Renovated R.C. beam	54.00	Beam: 16.257 Rebar: 101.490 FRP: -	15.00
L-1-3	A_s: 14mm rebar Status: Renovated R.C. beam with FRP composite	59.00	Beam: 17.175 Rebar: 101.77 FRP: 16.55	17.00

Table 1 show the parameter of the control beam (L-1-1, L-2-1) is approaching with the renovated beam (L-1-2, L-2-2) while the GFRP composite beam is advantage in load bearing performance compare with others. Furthermore, the R.C beam with 14mm diameter rebar (L-2-1, L-2-2, L-2-3) show superior in load bearing compare with 12mm diameter rebar R.C beam (L-1-1, L-1-2, L-1-3).

Table 2 Stress tensor of perpendicular beam with GFRP composite

Beam code	Description	Rupture load (kN)	Axial stress (MPa)	M_u(kN)
N-1-1	A_s: 12mm rebar Status: Control-R.C. beam	46.50	Beam: 15.440 Rebar: 103.150 FRP: -	11.37
N-1-2	A_s: 12mm rebar Status: Renovated R.C. beam	47.00	Beam: 15.650 Rebar: 103.260 FRP: -	11.39
N-1-3	A_s: 12mm rebar Status: Renovated R.C. beam with FRP composite	47.50	Beam: 15.655 Rebar: 103.320 FRP: 14.899	12.75
N-2-1	A_s: 14mm rebar Status: Control-R.C. beam	49.50	Beam: 15.712 Rebar: 103.330 FRP: -	15.24
N-2-2	A_s: 14mm rebar Status: Renovated R.C. beam	51.00	Beam: 16.229 Rebar: 103.610 FRP: -	15.27
N-1-3	A_s: 14mm rebar Status: Renovated R.C. beam with FRP composite	53.50	Beam: 17.067 Rebar: 101.060 FRP: 16.189	17.28

Table 2 show the parameter for the control beam (N-1-1, N-2-1) is approaching with the renovated beam (N-1-2, N-2-2) while the GFRP composite beam was show advantage in load bearing performance compare with others. Furthermore, the R.C beam with 14mm diameter rebar (N-2-1, N-2-2, N-2-3) was show superior in load bearing compare with 12mm diameter rebar R.C beam (N-1-1, N-1-2, N-1-3).

3.2 Plastics region in GFRP composite beam

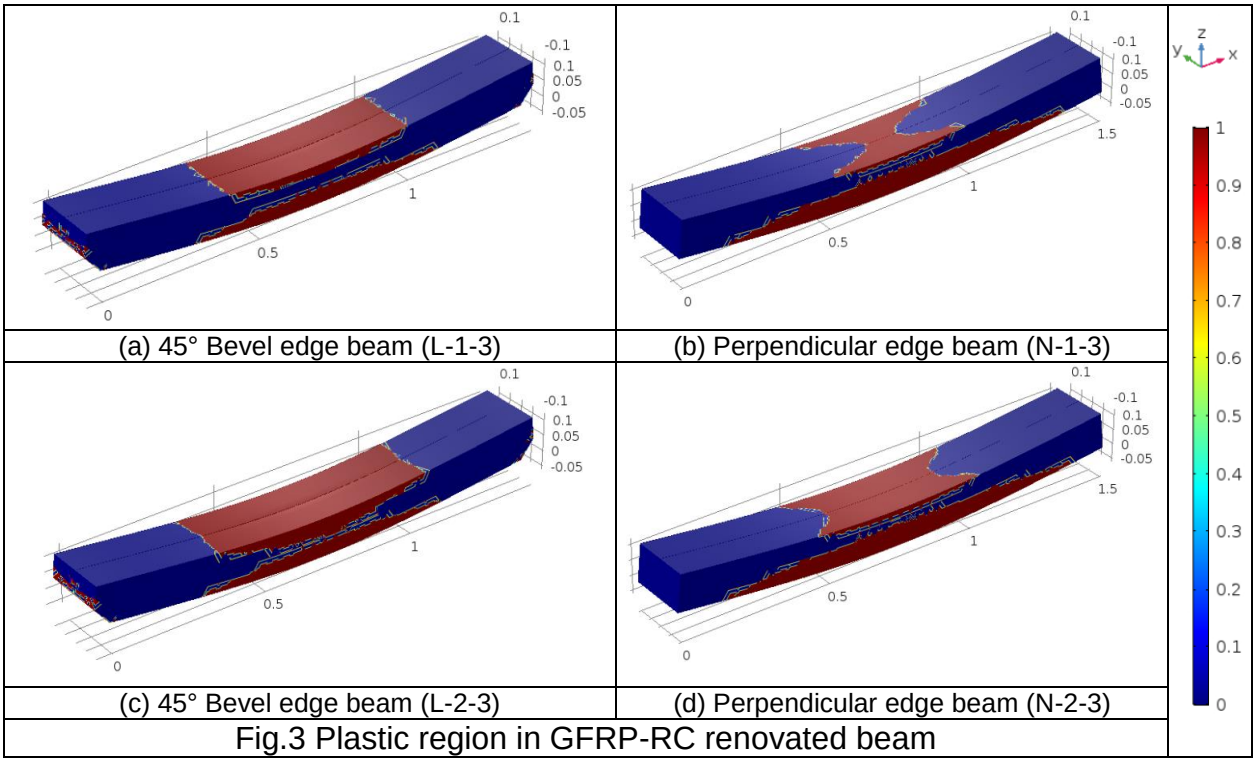

(a) 45° Bevel edge beam (L-1-3)

(b) Perpendicular edge beam (N-1-3)

(c) 45° Bevel edge beam (L-2-3)

(d) Perpendicular edge beam (N-2-3)

Fig.3 Plastic region in GFRP-RC renovated beam

Fig.3 show the particular plastic region for the distinct edge of GFRP-RC beam with the difference component of rebar diameter as 12mm and 14mm in the tensile strength A_s area respectively. Figs.3(a) and 3(c) represent the plasticity mode in 45° bevel edge beam at the soffit and force receiving area as well as the part of it bearing edge with the evenly plasticity status. Figs.3(b) and 3(d) show the uneven force receiving in the soffit and force receiving area. Where, the plasticity status as show in the tensile strength A_s at the soffit is larger than the forces receiving area. The result demonstrates that the variable shape form of the beam edge is a potential for load bearing increasing while the rupture status is not an identical performance for each beam. The material will continuance plasticity or irreversible deformation on tensile or compressive mode in case of exceeds a critical mode. The numerical formula of plasticity is depending on the Tresca and the von Mises criteria to determine the behavior of a material after receiving the bearing force as Eq.(8) indicated by (Ian Burgess 2017), (O.A. Bauchau and J.I.Craig 2009) and (W. M. Huang and X.Y. Gao 2004).

$$\sigma_v^2 = \frac{1}{2}[(\sigma_{11} - \sigma_{22})^2 + (\sigma_{22} - \sigma_{33})^2 + (\sigma_{11} - \sigma_{33})^2 + 6(\sigma_{23}^2 + \sigma_{31}^2 + \sigma_{12}^2)] \quad (8)$$

4. COMPARISION OF BEVEL EDGE BEAM AND PERPENDICULAR EDGE BEAM

Table 3 Simulation, calculation and experimental result in flexural strength

Beam code	45° Bevel edge beam					Beam code	Perpendicular edge beam		
	M_{ex} (kN·m)	M_{si} (kN·m)	M_{cal} (kN·m)	M_{ex}/M_{si}	M_{cal}/M_{si}		M_{si} (kN·m)	M_{cal} (kN·m)	M_{cal}/M_{si}
L-1-1	12.52	11.20	12.43	1.12	1.10	**N-1-1**	11.37	12.32	1.08
L-1-2	12.75	11.21	13.52	1.14	1.21	**N-1-2**	11.39	12.34	1.08
L-1-3	13.25	12.57	14.05	1.05	1.12	**N-1-3**	12.75	15.31	1.20
L-2-1	13.13	14.98	13.92	0.88	0.93	**N-2-1**	15.24	13.97	0.92
L-2-2	13.50	15.00	14.92	0.90	0.99	**N-2-2**	15.27	13.99	0.92
L-2-3	14.75	17.00	15.65	0.87	0.92	**N-2-3**	17.28	16.93	0.98

Table 3 shown the deviation of simulation result with experiment result ($\boldsymbol{M_{ex}/M_{si}}$) is approaching to 1.00 whereas the deviation of calculation result with simulation result ($\boldsymbol{M_{cal}/M_{si}}$) is identical approaching to 1.00. Hence, the flexural strength of both simulation and calculation result for 45°bevel edge beam is approaching with the experiment result for the flexural strength. Consequently, the deviation of calculation result with the simulation result ($\boldsymbol{M_{cal}/M_{si}}$) for the perpendicular edge beam is show identical disparity while the simulation modeling and calculation formula as indicated from Eqs.(1)-(7) is satisfying to be a perdition method for GFRP-RC composite beam depend on the verification result from the 45° bevel edge beam experiment data.

5. CONCLUSIONS

The prediction of renovated beam with GFRP-RC composite material in 45° bevel edge is present in simulation model and numerical calculation in verification with the experiment result to obtain the disparity of flexural strength. Moreover, to predict the intensity of variable geometry form between 45° bevel edge beam and perpendicular edge beam in load carrying. The result show that:

- The prediction of simulation numerical in bevel edge beam with BEM method is practical and satisfy for flexural strength result.
- The load bearing of 45° bevel edge beam is significant advantage in compare with the perpendicular edge beam. Whereas, the renovated beam with GFRP-RC beam is signification for component coordination in load bearing compare with the perpendicular edge beam.
- Prediction for plastic region show obviously in rupture status for the 45° bevel edge beam after loading bearing.
- The modification formula is successful to calculated the variable perimeter after beam renovated with the composition of GFRP.

ACKNOWLEDGMENTS

The author would like to acknowledge the High-level Talent Project Funding Scheme of Jiangsu (JZ-010), Post-doctoral fund of China and Jiangsu (1301057B, 2014M551588) and the Fundamental research funds for the Central universities (NS2015010) for its financial support in this project.

REFERENCES

Axiang Zhu (2017), “Force analysis and numerical simulation on reinforced concrete segment”, Master Dissertation, Nanjing University of Aeronautics and Astronautics’, Nanjing.

ACI 440.2R-08. (2008) “Guide for the design and construction of externally bonded FRP systems for strengthening concrete structures”. *American Concrete Institute*.

Hind M. Kh., Mustafa Özakça, Talha Ekmekyapar and Abdolbaqi M. Kh. (2016), “Flexural behavior of concrete beams reinforced with different types of fibers”, *Computers and Concrete* **18**(5) 999-1018

Hany J.Z, Felipe Mejia, Antonio Nanni (2013). “Strength reduction factor for flexural RC members strengthened with near-surface-mounted bars”. *Journal composite construction*; **17**(5):614-625.

Liang Jiongfeng, Yu Deng, Yang Zeping and Chai Xinjun (2016)*, “*Tests of concrete slabs reinforced with CFRP prestressed prisms*” Computers and Concrete* **18**(3) 355-366

Anand Ganganogoudar, Tarutal Ghosh Mondal and S. Suriya Prakash (2016). “Analytical and finite element studies on behavior of FRP strengthened RC beam under torsion”. *Composite Structures*; **153**(2016)876-885.

Zhang Dongliang, Wang Qingyuan and Dong Jiangfeng (2016), “Simulation study on CFRP strengthened reinforced concrete beam under four-point bending” *Computers and Concrete* **17**(3) 407-421

COMSOL Multiphysics (1988-2016), “Concrete beam with reinforcement bars”, *COMSOL Multiphysics 5.2a*, cn.comsol.com.

Ian Burgess (2017), “Yield-line plasticity and tensile membrane action in lightly-reinforced rectangular concrete slabs”. *Engineering Structures* **138**(2017) 195-214.

O.A. Bauchau and J.I.Craig (2009), *Structural Analysis with Application to Aerospace Structures*, Springer Science and Business Media B.V., New York, USA.

W. M. Huang and X.Y. Gao (2004), “Tresca and von Mises yield criteria: a view from strain space”. *Philosophical magazine letters* **84**(10) 625–629.